siRNA delivery

Deutsche Ausgabe: DOI: 10.1002/ange.201601441
Internationale Ausgabe: DOI: 10.1002/anie.201601441

In Situ Functionalized Polymers for siRNA Delivery

Juan M. Priegue, Daniel N. Crisan, José Martínez-Costas, Juan R. Granja, Francisco Fernandez-Trillo, and Javier Montenegro**

Abstract: *A new method is reported herein for screening the biological activity of functional polymers across a consistent degree of polymerization and in situ, that is, under aqueous conditions and without purification/isolation of candidate polymers. In brief, the chemical functionality of a poly(acryloyl hydrazide) scaffold was activated under aqueous conditions using readily available aldehydes to obtain amphiphilic polymers. The transport activity of the resulting polymers can be evaluated in situ using model membranes and living cells without the need for tedious isolation and purification steps. This technology allowed the rapid identification of a supramolecular polymeric vector with excellent efficiency and reproducibility for the delivery of siRNA into human cells (HeLa-EGFP). The reported method constitutes a blueprint for the high-throughput screening and future discovery of new polymeric functional materials with important biological applications.*

Polymers are emerging as one of the most promising scaffolds for the multivalent presentation of relevant biological information.[1,2] Polymeric displays of chemical motifs trigger new opportunities for cargo conjugation and delivery of the resulting covalent and/or supramolecular nanocomposites.[3] Polymers have been suggested as one of the best nanomaterials for drug delivery.[3,4] Along these lines, the delivery of exogenous small interfering RNA (siRNA)[5,6] is one potential therapy where polymers have attracted great attention.[7] RNA interference (RNAi) can regulate gene expression in a catalytic manner, and as such, offers several advantages over other gene therapies.[8] However, the potential biosafety problems associated with viral vectors and the intrinsic limitations of siRNA (for example, nuclease digestion) strongly hinder the development of suitable therapies.[6] It is therefore crucial to innovate and to identify new synthetic vectors for the delivery of functional polynucleotides.

Current progress in polymer synthesis allows the preparation of materials with multiple functionalities capable of mimicking some of the desired characteristics of viral vectors for gene delivery.[7,9] To speed up this discovery process, screening strategies have been developed.[10–14] However, in most of these cases the monomer composition strongly affects the outcome of the polymerization results.[15] Furthermore, these platforms are often compromised by the lack of strategies that allow evaluation of a range of chemical compositions across a consistent molecular weight and/or polymer length. Moreover, there are even fewer procedures that allow the in situ evaluation of the generated polynucleotide vectors.[12] Therefore, purification/isolation steps have to be implemented, even for inactive candidates, increasing the time required and the cost of the discovery process. Unfortunately, as the sophistication in polymer design increases, so does the synthetic effort required to prepare polymer vectors.

In this Communication we report the synthesis of poly(acryloyl hydrazide)s for their straightforward functionalization with aldehydes to afford amphiphilic polymers that can be screened in situ (that is, under aqueous conditions and without further purification) for the activated transport of nucleotides across lipid membranes (Scheme 1). Optimization of these hydrazone-activated polymers can be performed under aqueous conditions and without purification, minimizing the synthetic effort and the time required to identify novel candidates for polynucleotide delivery. This versatile technology allowed the rapid identification of a single component formulation for the delivery of siRNA with better performance than one of the best commercial reagents (lipofectamine RNAiMAX).

Post-polymerization functionalization is an ideal strategy to develop and to evaluate polymer compositions across a consistent degree of polymerization.[16] Post-polymerization often relies on highly efficient reactions (such as cycloadditions, reversible carbonyl chemistry, thiol-ene) to modify polymer properties.[16] Of these, we anticipated that using a poly(acryloyl hydrazide) scaffold (**P1**, Scheme 1) would give the required solubility in water to be able to screen for siRNA delivery without the need to purify the candidate amphiphiles. Poly(hydrazides) are weakly protonated at neutral pH[10] and can readily react with aldehydes to form acyl hydrazones that are sufficiently stable under physiological conditions.[17] Accordingly, hydrazone formation has been widely used in biological settings including drug delivery,[18] sensing,[19,20] or even in the synthesis of polynucleotide delivery vectors.[21,22] However, the use of poly(hydrazide) as a "clickable" and versatile scaffold has been limited and only a few examples report its use to synthesize glycopolymers or for pH-

[*] J. M. Priegue, Prof. Dr. J. R. Granja, Dr. J. Montenegro
Departamento de Química Orgánica
Centro Singular de Investigación en Química Biolóxica e Materiais Moleculares (CIQUS)
Universidade de Santiago de Compostela E-15782 (Spain)
E-mail: javier.montenegro@usc.es
Dr. J. Martínez-Costas
Departamento de Bioquimica y Biología Molecular
Centro Singular de Investigación en Química Biolóxica e Materiais Moleculares (CIQUS)
Universidade de Santiago de Compostela E-15782 (Spain)
D. N. Crisan, Dr. F. Fernandez-Trillo
School of Chemistry, University of Birmingham
B15 2TT (UK)
E-mail: f.fernandez-trillo@bham.ac.uk

Supporting information and the ORCID identification number(s) for the author(s) of this article can be found under http://dx.doi.org/10.1002/anie.201601441.

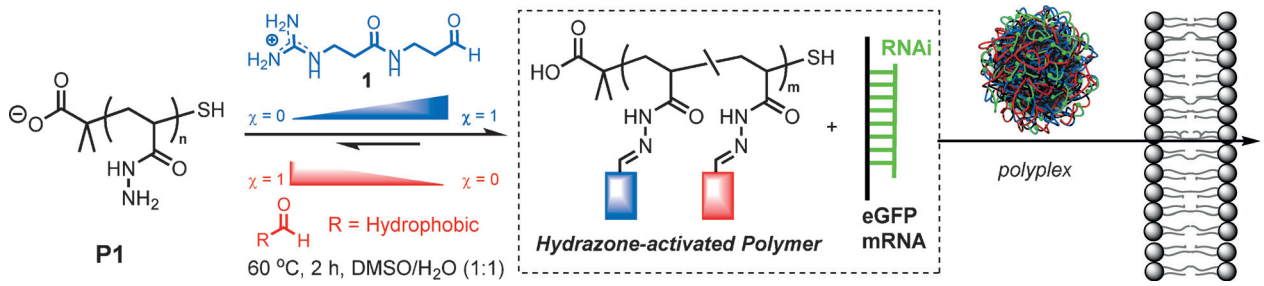

Scheme 1. Post-polymerization functionalization with cationic and hydrophobic aldehydes is followed by supramolecular conjugation of activated polymers with cargo (siRNA) and polyplex delivery. χ = molar fraction.

responsive drug delivery.[16,23,24] Alternative elegant strategies for multi-hydrazone formation have also been developed in the context of DNA or protein-templated dynamic combinatorial libraries.[25–28]

The proposed poly(acryloyl hydrazide) scaffold (**P1**) was prepared using controlled free radical polymerization (see the Supporting Information). **P1** was highly water soluble and aqueous hydrazone formation was readily confirmed by employing the UV-active 4-imidazolecarboxaldehyde. ^{1}H NMR spectroscopic analysis of **P1** incubated (for less than 1 h) with 4-imidazolecarboxaldehyde (0.3–0.9 equiv in 100 mM AcOH in D_2O) showed a broadening of the aromatic proton resonance signals of the aldehyde (see Figure S3 in the Supporting Information). Comparison of the residual aldehyde signal against the overall amount of protons revealed that the loading of 4-imidazolecarboxaldehyde on **P1** was about 70% (Figure S3).[23] No increase in loading was detected with a higher number of equivalents of aldehyde, longer times (up to 4 h), different solvents, or even with heating. Further characterization was obtained from gel permeation chromatography (GPC; Figure 1). A clear peak for the polymer **P1**(**Imidazole**) (retention time R_t = 18 min) was already detected with only 0.25 equiv of 4-imidazolecarboxaldehyde added to **P1**, confirming attachment of the chromophore to **P1** (Figure 1). Increasing amounts of 4-imidazolecarboxaldehyde resulted in an increase in the intensity of the peak at 18 min, with the signal reaching a maximum at around 0.75 equiv. Further equivalents simply increased the amount of free 4-imidazolecarboxaldehyde (R_t = 31 min), validating the NMR estimation of a maximum polymer loading of about 70% (Figure S3).

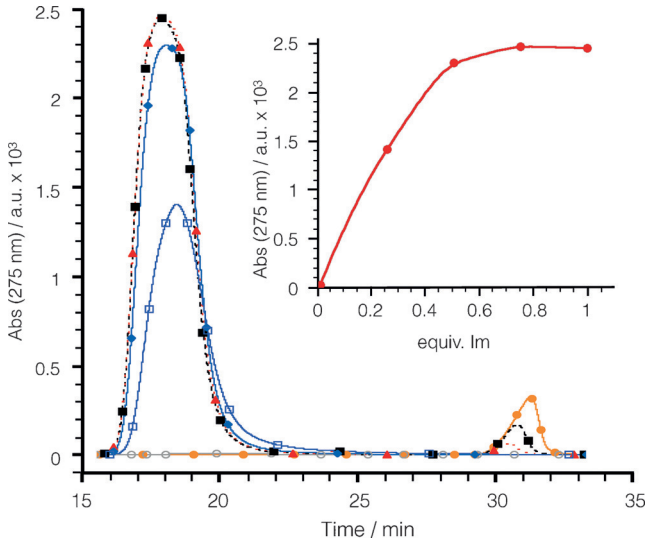

Figure 1. GPC (λ_{Abs} = 275 nm) analysis of **P1** incubated with 1 (black ■), 0.75 (red ▲), 0.5 (blue ◆), 0.25 (purple □), or 0 (gray ○) equiv of 4-imidazolecarboxaldehyde. The spectrum for pure 4-imidazolecarboxaldehyde (orange ●) is also shown. Conditions: 100 mM acetic acid, pH 2.9, 2 h. Inset: Increase in absorbance of the high molecular weight peak (R_t = 18 min) with increasing amounts of 4-imidazolecarboxaldehyde.

Having established the feasibility of modifying **P1** with a model aldehyde, we explored the use of **P1** for the in situ screening of membrane-active polymers. A close inspection of some of the structural motifs commonly found in membrane-active polymers (for example antimicrobial or cell-penetrating polymers) highlights a high prevalence of amphiphilic structures with the presence of both cationic (such as guanidinium) and hydrophobic moieties (such as isopropyl or benzyl).[19,29,30] The potential of establishing bidentate hydrogen bonding and stable protonation under physiological conditions makes the guanidinium group ($pK_a \approx 12.5$) the optimal cationic moiety for membrane penetration. Thus, we decided to investigate a small library of aldehydes where the cationic aldehyde (**1**, Scheme 1) was kept constant and independently combined with different hydrophobic aldehydes (Figure 2; see also the Supporting Information).

Activated polymers for membrane transport were thus prepared by combining an aqueous stock solution of **P1** with a DMSO solution containing the cationic and the corresponding hydrophobic aldehydes in different molar ratios (see the Supporting Information for details). Hydrazone formation of **P1** with long hydrophobic aldehydes ($\geq$ 8 carbon atoms) lead to the rapid precipitation of the resulting polymers, making these combinations inappropriate for further evaluation. However, the combination of a series of short hydrophobic aldehydes (for example isovaleraldehyde (**2**)) with **1** afforded water-soluble and stable polyhydrazone nanoparticles (Figure S4). Dynamic light scattering (DLS) analysis revealed suitable sizes for membrane transport (about 200 nm) at a molar ratio of cationic/hydrophobic aldehydes = 0.85:0.15 (Figures S4 and S17).[21] Neighboring effects (i.e. cation repulsion) could impact the final composition of the final hydrazone-modified polymer. Therefore, to further characterize the post-polymerization reaction, we measured the DLS properties and the zeta potential of **P1** combined with different ratios of guanidinium aldehyde (**1**) and isovaleraldehyde (**2**). These measurements showed that increasing the molar fraction of hydrophobic aldehyde increased the size

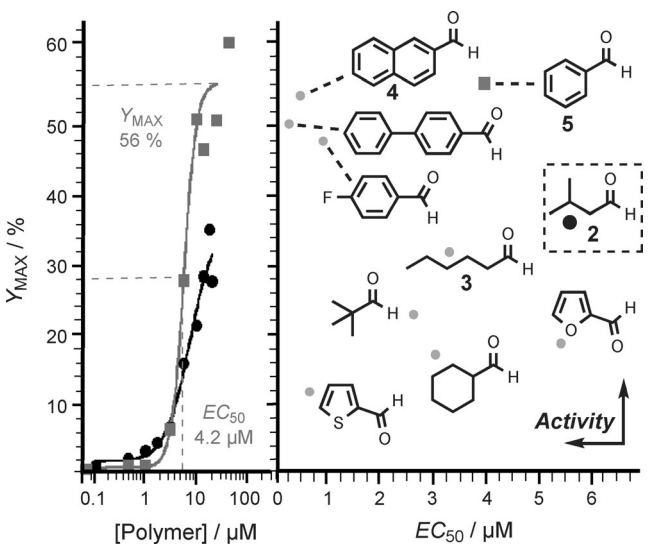

Figure 2. Y_{MAX} values versus polymer concentration (left) or versus EC_{50} (half maximal effective concentrations; right) for the DNA transport experiments in EYPC-LUVs⊃HPTS/DPX for hydrazone-activated polymers at χ(Hydrophobic) = 0.15 and χ**1** = 0.85. In the left plot, **5** (squares) and **2** (circles) are employed as the hydrophobic aldehydes.

and thus the cationic character of the resulting polymeric nanoparticles (Figure S4b). The maximum increase was detected at a molar fraction of **2** of χ**2** = 0.3–0.4, with further increases causing an important decrease in both the size and the zeta potential (Figure S4B). These results confirmed that changes in the aldehyde molar ratios are directly translated into the composition of the hydrazone-modified polymer.

Lead hydrazone-activated polymers from DLS analysis were then evaluated in supramolecular DNA transport experiments using large unilamellar vesicles (egg yolk L-α-phosphatidylcholine (EYPC LUVs)) loaded with 8-hydroxypyrene-1,3,6-trisulfonic acid trisodium salt and *p*-xylene-bis-pyridinium bromide (EYPC LUVs⊃HPTS/DPX).[19,20] This routine assay reports the release of internal dye molecules as an increase in the fluorescence of HPTS (Figure S5). This model allows the quick identification of inactive formulations as well as compositions that lead to significant membrane damage. In these experiments, a heterogeneous mixture of short double-stranded DNA molecules (dsDNAs; herring DNA) was selected to model siRNA. Transport experiments in these fluorogenic vesicles revealed isovaleraldehyde (**2**) and hexanal (**3**), and 2-naphthaldehyde (**4**) and benzaldehyde (**5**), as the leading hits for the aliphatic and the aromatic series, respectively (Figure 2; Figure S8, Table S2). Increasing the molar fraction of hydrophobic aldehydes over 0.15 (χ(Hydrophobic) > 0.15) afforded amphiphilic polymers with membrane-disrupting behaviors (Figure S6). Control experiments confirmed a lack of activity for the parent hydrazide **P1** either pure or independently combined with hydrophilic (**1**) or hydrophobic aldehydes (Figure S7).

Following the synthesis and in situ screening of polyhydrazones for membrane activity and DNA transport, the aldehyde lead candidates from fluorogenic assays, **2**, **3**, **4**, and **5**, were taken forward for their evaluation in siRNA delivery (EGFP (enhanced green fluorescent protein) gene knockdown) in HeLa-EGFP cells (Figure 3; see the Supporting Information for details).[31] Again, isolation and purification of the synthesized activated polymers was not required and transfection experiments were performed by simply diluting freshly prepared polyhydrazones (buffer/DMSO; see the Supporting Information for details) in culture media. In these experiments, activated polymers with aldehydes **3**, **4**, and **5** showed no activity for siRNA delivery in cells (Figure S11). Aliphatic isovaleraldehyde (**2**), however, showed efficient EGFP knockdown with an accurate reproducibility in all the transfection replicates measured (Figures S9–S14).

The biocompatible experimental conditions for the preparation of hydrazone-activated polymers allowed the straightforward optimization of this polymeric vector. We evaluated **P1** with different molar ratios of isovaleraldehyde (χ**2** = 0–0.4) and different polymer concentrations to maximize transfection efficiency and cell viability (Figure 3; Figure S15). Interestingly, the optimum molar ratio of the hydrophobic aldehyde (χ**2** = 0.15; Figure 3A) correlated well with the molar ratio identified in vesicle transport experiments (Figure 2; Figures S6, S8). Maximum transfection efficiency for **P1**(**1**)$_{85}$(**2**)$_{15}$ (where the subindices indicate the percentage of the corresponding aldehyde) could be achieved at a concentration of 4 μM (Figure S12). Under these conditions, we could confirm the formation of supramolecular polyplexes (150 nm) with a positive ζ-potential of +7 mV (Figure S17). Additionally, gel electrophoresis showed complete complexation of RNA into the polymeric polyplexes with as little as 0.12 μM of **P1**(**1**)$_{85}$(**2**)$_{15}$ (Figure S18).

Cell viability was optimal for the parent polymer **P1** and for the entire range of molar fractions and concentrations of the active **P1**(**1**)$_{85}$(**2**)$_{15}$ (Figure 3A; Figures S15, S16). However, increasing the molar ratio of the hydrophobic aldehyde (χ**2** = 0.4) caused a slight decrease in cell viability together

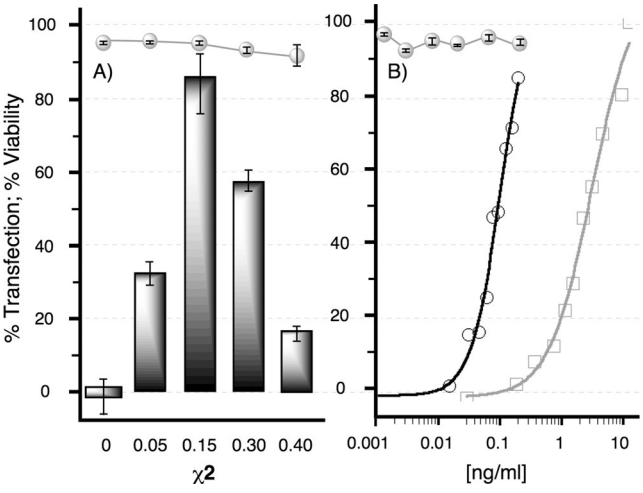

Figure 3. A) Transfection efficiency (bars) and cell viability (circles) in HeLa-EGFP cells at constant siRNA (14 nM) and **P1**(**1**)$_{85}$(**2**)$_{15}$ (4 μM) concentrations and prepared with different molar fractions of **2**. B) Dose–response curves of lead candidate **P1**(**1**)$_{85}$(**2**)$_{15}$ (empty circles; EC_{50} = 0.09 ng mL^{-1}) and Lipofectamine RNAiMAX (empty squares; EC_{50} = 2.5 ng mL^{-1}), as well as the percentage cell viability for **P1**(**1**)$_{85}$(**2**)$_{15}$ (gray filled circles, top).

with an increase in the standard deviation of the assay (Figure 3A, circles). This observation could be related with the membrane detergent behavior detected for highly hydrophobic polyhydrazones in vesicle experiments (Figure 3A; Figure S15, Figure S6). Remarkably, a comparison of the dose–response curves of transfection efficiency revealed that the polymeric vector performed with almost equal efficiency using a concentration more than ten times less than that of the commercial reagent lipofectamine RNAiMAX (Figure 3B). Furthermore, the stability of all the components involved in the preparation of this polymeric cytofectin allowed the storage of the stock solutions for months while keeping intact their transfection efficiency.

In conclusion, we have developed a novel strategy for the in situ evaluation (that is, under aqueous conditions and without purification) of polymers with biological activity. Poly(hydrazide) functionality has been "activated", under aqueous conditions, to yield amphiphilic functional polymers that did not require any further purification for their evaluation in relevant biological assays. This procedure allowed the rapid identification of a single-component supramolecular polymeric formulation for siRNA transfection with better performance than the current gold standard for siRNA delivery. We believe that the reported method is not limited to the screening of polynucleotide delivery and that it can be easily adapted (through an informed choice of aldehydes) for the high-throughput screening of polymers with complex chemical functionalities and different biological relevance. The control over the distribution and sequential arrangement of the aldehyde groups onto the polymer scaffold will be a great future challenge that will allow the investigation of intriguing topology/activity relationships. Our efforts in these directions will be reported in due course.

Acknowledgements

This work was supported by the Royal Society, U.K (IE130688) and the Spanish Ministry of Economy and Competitiveness (CTQ2014-59646-R, CTQ2013-43264-R, and BFU2013-43513-R). We thank Rebeca Menaya-Vargas for assistance with cell protocols. F.F.-T. thanks the Birmingham Science City and the European Regional Development Fund, the Royal Society (RG140273), and the University of Birmingham for a John Evans Fellowship. J.M.P. received an F.P.I. contract from MEC. J.M. received a Ramon y Cajal from MINECO and a Starting Grant from the ERC (DYNAP-677786).

Keywords: lipid bilayer membranes · polymers · siRNA delivery · supramolecular chemistry · vesicles

How to cite: *Angew. Chem. Int. Ed.* **2016**, *55*, 7492–7495
Angew. Chem. **2016**, *128*, 7618–7621

[1] S. F. M. van Dongen, H.-P. M. de Hoog, R. J. R. W. Peters, M. Nallani, R. J. M. Nolte, J. C. M. van Hest, *Chem. Rev.* **2009**, *109*, 6212–6274.
[2] C. S. Mahon, D. A. Fulton, *Nat. Chem.* **2014**, *6*, 665–672.
[3] J. Nicolas, S. Mura, D. Brambilla, N. Mackiewicz, P. Couvreur, *Chem. Soc. Rev.* **2013**, *42*, 1147–1235.
[4] M. W. Tibbitt, J. E. Dahlman, R. Langer, *J. Am. Chem. Soc.* **2016**, *138*, 704–717.
[5] M. E. Davis, J. E. Zuckerman, C. H. J. Choi, D. Seligson, A. Tolcher, C. A. Alabi, Y. Yen, J. D. Heidel, A. Ribas, *Nature* **2010**, *464*, 1067–1070.
[6] J.-P. Behr, *Acc. Chem. Res.* **2012**, *45*, 980–984.
[7] K. Miyata, N. Nishiyama, K. Kataoka, *Chem. Soc. Rev.* **2012**, *41*, 2562–2574.
[8] R. C. Mulligan, *Science* **1993**, *260*, 926–932.
[9] T. Wang, J. R. Upponi, V. P. Torchilin, *Int. J. Pharm.* **2012**, *427*, 3–20.
[10] M. P. Xiong, Y. Bae, S. Fukushima, M. L. Forrest, N. Nishiyama, K. Kataoka, G. S. Kwon, *ChemMedChem* **2007**, *2*, 1321–1327.
[11] J. J. Green, R. Langer, D. G. Anderson, *Acc. Chem. Res.* **2008**, *41*, 749–759.
[12] S. Barua, A. Joshi, A. Banerjee, D. Matthews, S. T. Sharfstein, S. M. Cramer, R. S. Kane, K. Rege, *Mol. Pharm.* **2009**, *6*, 86–97.
[13] A. C. Rinkenauer, L. Tauhardt, F. Wendler, K. Kempe, M. Gottschaldt, A. Traeger, U. S. Schubert, *Macromol. Biosci.* **2015**, *15*, 414–425.
[14] J. Hao, P. Kos, K. Zhou, J. B. Miller, L. Xue, Y. Yan, H. Xiong, S. Elkassih, D. J. Siegwart, *J. Am. Chem. Soc.* **2015**, *137*, 9206–9209.
[15] D. M. Lynn, D. G. Anderson, D. Putnam, R. Langer, *J. Am. Chem. Soc.* **2001**, *123*, 8155–8156.
[16] M. A. Gauthier, M. I. Gibson, H.-A. Klok, *Angew. Chem. Int. Ed.* **2008**, *48*, 48–58; *Angew. Chem.* **2008**, *121*, 50–60.
[17] J. Kalia, R. T. Raines, *Angew. Chem. Int. Ed.* **2008**, *47*, 7523–7526; *Angew. Chem.* **2008**, *120*, 7633–7636.
[18] C. C. Lee, E. R. Gillies, M. E. Fox, S. J. Guillaudeu, J. M. J. Fréchet, E. E. Dy, F. C. Szoka, *Proc. Natl. Acad. Sci. USA* **2006**, *103*, 16649–16654.
[19] T. Takeuchi, V. Bagnacani, F. Sansone, S. Matile, *ChemBioChem* **2009**, *10*, 2793–2799.
[20] J. M. Priegue, J. Montenegro, J. R. Granja, *Small* **2014**, *10*, 3613–3618.
[21] C. Gehin, J. Montenegro, E.-K. Bang, A. Cajaraville, S. Takayama, H. Hirose, S. Futaki, S. Matile, H. Riezman, *J. Am. Chem. Soc.* **2013**, *135*, 9295–9298.
[22] C. Bouillon, D. Paolantoni, J. C. Rote, Y. Bessin, L. W. Peterson, P. Dumy, S. Ulrich, *Chem. Eur. J.* **2014**, *20*, 14705–14714.
[23] K. Godula, C. R. Bertozzi, *J. Am. Chem. Soc.* **2010**, *132*, 9963–9965.
[24] A. Kumar, R. R. Ujjwal, A. Mittal, A. Bansal, U. Ojha, *ACS Appl. Mater. Interfaces* **2014**, *6*, 1855–1865.
[25] C. S. Mahon, D. A. Fulton, *Chem. Sci.* **2013**, *4*, 3661–3666.
[26] C. S. Mahon, M. A. Fascione, C. Sakonsinsiri, T. E. McAllister, W. Bruce Turnbull, D. A. Fulton, *Org. Biomol. Chem.* **2015**, *13*, 2756–2761.
[27] E. Bartolami, Y. Bessin, V. Gervais, P. Dumy, S. Ulrich, *Angew. Chem. Int. Ed.* **2015**, *54*, 10183–10187; *Angew. Chem.* **2015**, *127*, 10321–10325.
[28] C. S. Mahon, A. W. Jackson, B. S. Murray, D. A. Fulton, *Chem. Commun.* **2011**, *47*, 7209–7211.
[29] K. Lienkamp, G. N. Tew, *Chem. Eur. J.* **2009**, *15*, 11784–11800.
[30] F. Sgolastra, B. M. deRonde, J. M. Sarapas, A. Som, G. N. Tew, *Acc. Chem. Res.* **2013**, *46*, 2977–2987.
[31] C. Piñero-Lambea, G. Bodelón, R. Fernández-Periáñez, A. M. Cuesta, L. Álvarez-Vallina, L. Á. Fernández, *ACS Synth. Biol.* **2015**, *4*, 463–473.

Received: February 9, 2016
Published online: April 21, 2016

